Developmental Cell, Volume *21*

Supplemental Information

Dlg3 Trafficking and Apical Tight Junction Formation Is Regulated by Nedd4 and Nedd4-2 E3 Ubiquitin Ligases

Claude A. Van Campenhout, Andrea Eitelhuber, Christian J. Gloeckner, Patrizia Giallonardo, Moritz Gegg, Heide Oller, Seth G. N. Grant, Daniel Krappmann, Marius Ueffing, and Heiko Lickert

Inventory of Supplemental Information

The Supplemental Information contains six Supplemental Figures and Supplemental Experimental Procedures. The Supplemental Figures provide supporting information for the data presented in the main figures, as follows:

Figure S1 is related to Figure 1 and demonstrates that loss of *Dlg3* leads to low penetrance embryonic lethality. Additionally, this figure shows Dlg3 contribution to planar cell polarity in the inner ear.

Figure S2 is related to Figure 2 and provides more data on loss of cell polarity in *Dlg3* mutants. Moreover, this figure present chimera analysis suggesting that Dlg3 acts cell autonomously in the axial mesendoderm and definitive endoderm lineages.

Figure S3 is related to Figure 3 and show the heterogeneous expression profile of the Dlgs in the mouse embryo.

Figure S4 is related to Figure 4 and presents Dlg3 localization in the cytoplasm and membrane of non polarized cells. This figure also shows the fast recruitment of Dlg3 to the apical plasma membrane and forming tight junctions in a re-polarization assay.

Figure S5 is related to Figure 5 and shows the alignment of the *Drosophila* Dlg and the mammalian Dlgs showing the presence of the PY motifs only in Dlg3.

Figure S6 is related to Figure 6 and provides more data on Dlg3 monoubiquitination by Nedd4. Also provided is evidence in MDK cells that SF-Dlg3^{YA1+2} blocks normal cysts polarization. Finally, this figure demonstrates that the combined Nedd4 and Nedd4-2 knock down does not affect AJ formation.

Supplemental Experimental procedures describe Tandem affinity purification and LC-MS/MS, generation of expression vectors, whole-mount *in situ* hybridizations, RT-PCR and cell culture procedures.

Figure S1, related to Figure 1

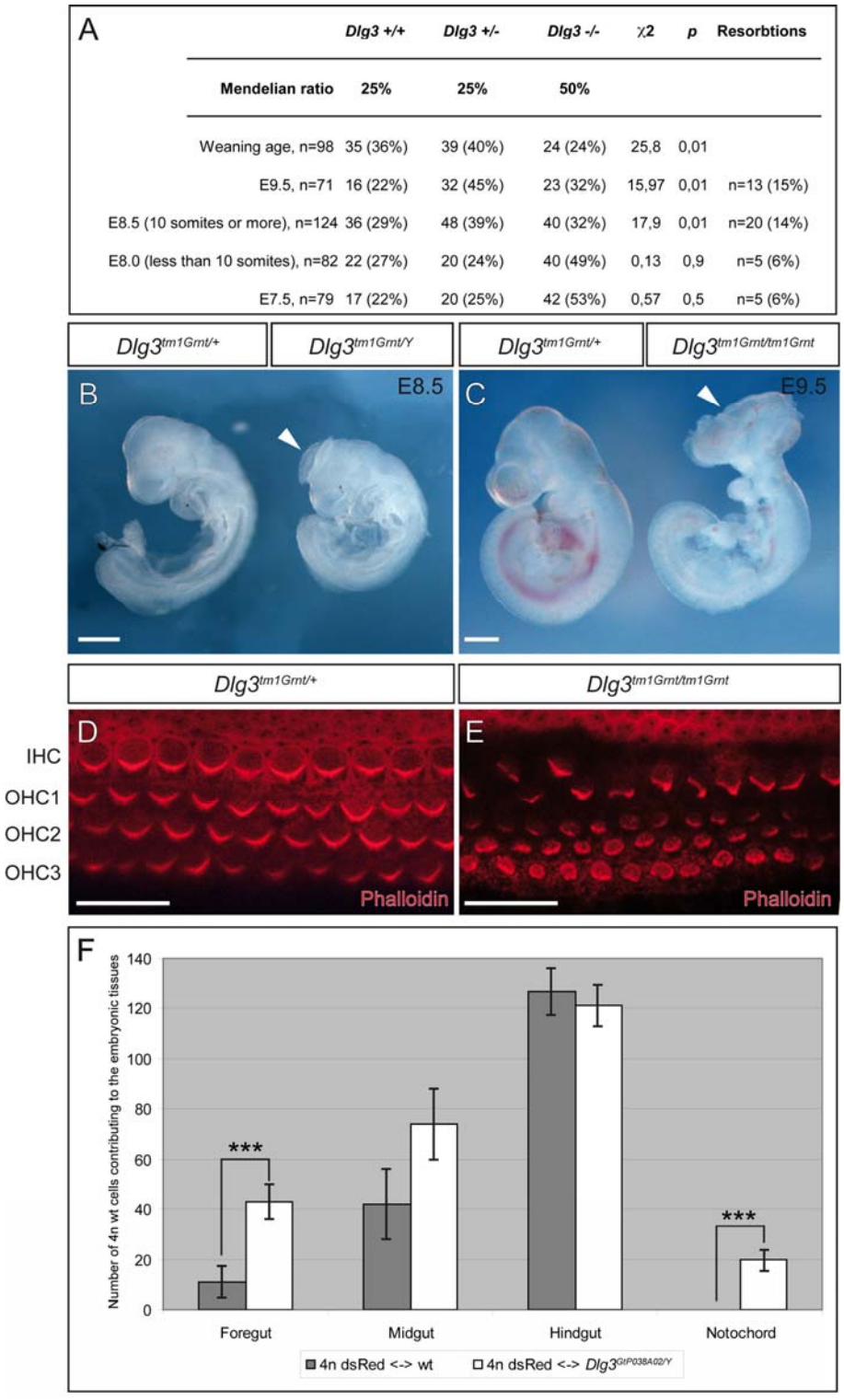

Figure S1. Loss of Dlg3 leads to low penetrant embryonic lethality and planar cell polarity defects

(A) *Dlg3* homozygous mutants show low penetrant embryonic lethality**.** Crosses between hemizygous males and heterozygous females produced null animals at a lower proportion

than the mendelian ratio. The chi-square test revealed that the difference in the frequency of *Dlg3* mutants at developmental stage E8.5 and onwards is statistically significant ($p<0.01$). There is no obvious skew in the male/female ratio in the surviving *Dlg3* KO animals (11 males/13 females).

(**B-C**) *Dlg3* null embryos show occasionally an open brain phenotype (n=8 out of 38; Figure S1B-C) and a forebrain deletion phenotype (n=6 out of 38, see Figure 1A-B).

(**D-E**) Apical view of the organ of Corti at E18.5 showing the sensory cilia bundles stained with phalloidin. In comparison to WT (**D**) *Dlg3* homozygous mutants (**E**) present disorganized and misoriented inner hair cells (n=6 out of 11 organs of Corti). IHC, inner hair cells; OHC, outer hair cells. Scale bars = 300µm in (**B-C**) and 20µm in (**D-E**).

(**F**) Quantification of the number of 4n wt cells contributing to the gut and notochord in 4n dsRed <-> wt (n=29) and 4n dsRed <-> $Dlg3^{GtP038A02/Y}$ chimeras (n=29) at E8.5-E9.0. Mean ± SD; *** $p<0.01$. n= 17, 22, 28 and 11 embryos counted for fore-, mid-, hindgut and notochord, respectively. Error bars indicate standard deviation.

Figure S2, related to Figure 2

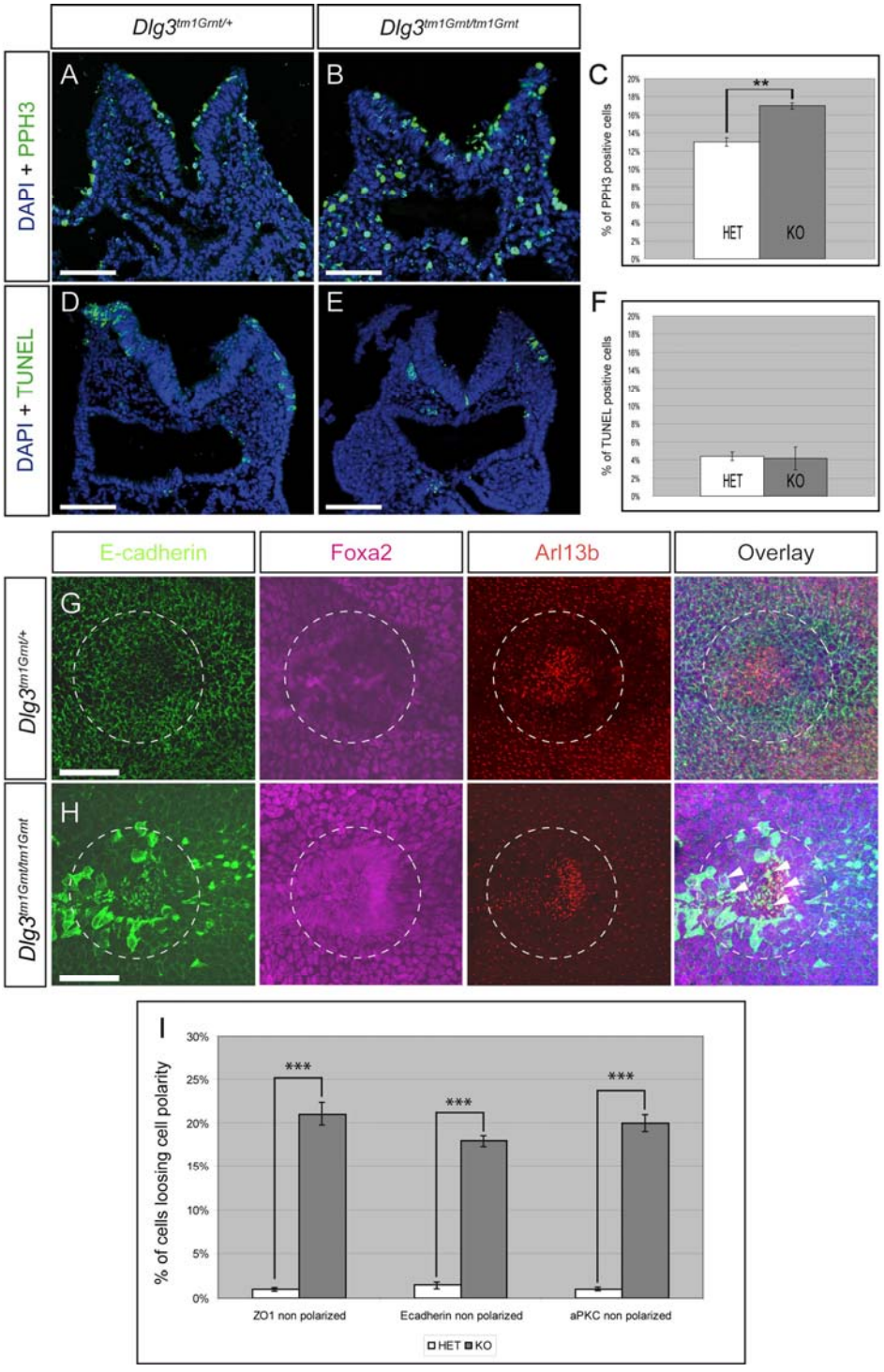

Figure S2. *Dlg3* inactivation leads to loss of cell polarity in the node region

(**A-B**) Mitotic cells were labelled with anti-phospho-histone H3 antibody (PPH3; green) and nuclei stained with DAPI on transverse sections of control and *Dlg3* homozygous mutants at E8.5-9.0. Scale bars = 100µm.

(**C**) Proliferation rate is significantly increased in *Dlg3* null embryos in comparison to controls. Mean values ± SD, 12 embryos were used for each genotype; control n= 4052, *Dlg3* null n= 4726 , ** $p<0.05$. Error bars indicate standard deviation.

(**D-E**) Apoptotic cells were labelled by TUNEL reaction (green) and nuclei stained with DAPI on transverse sections of control and *Dlg3* homozygous mutants at E8.5-9.0. Scale bars = 100µm.

(**F**) Apoptosis is not increased in *Dlg3* null embryos in comparison to controls. Mean values ± SD, 10 embryos were used for each genotype; control n= 5306, *Dlg3* null n= 5237. Error bars indicate standard deviation.

(**G-H**) Confocal images of whole-mount antibody stained embryos. Ventral views of the node region (outlined by dashed ovals) in (**G**) control and (**H**) *Dlg3* homozygous mutant embryos with the anterior facing left at E8.5. Embryos were stained with DAPI (blue) and with E-cadherin (green), Foxa2 (purple) and Arl13b (red) antibodies. Note the loss of basolateral localization of the AJ marker E-cadherin in *Dlg3* mutant $Foxa2^{+}$ ciliated node cells indicated by arrowheads. Scale bars= 50µm.

(**I**) Quantification of cell polarity loss in *Dlg3* homozygous mutant in the node region at E8.5. Mean values ± SD, *** $p<0.01$. n= 11, 13, 8, 10, 9 and 9 embryos used per marker in sequential left to right order.

Figure S3, related to Figure 3

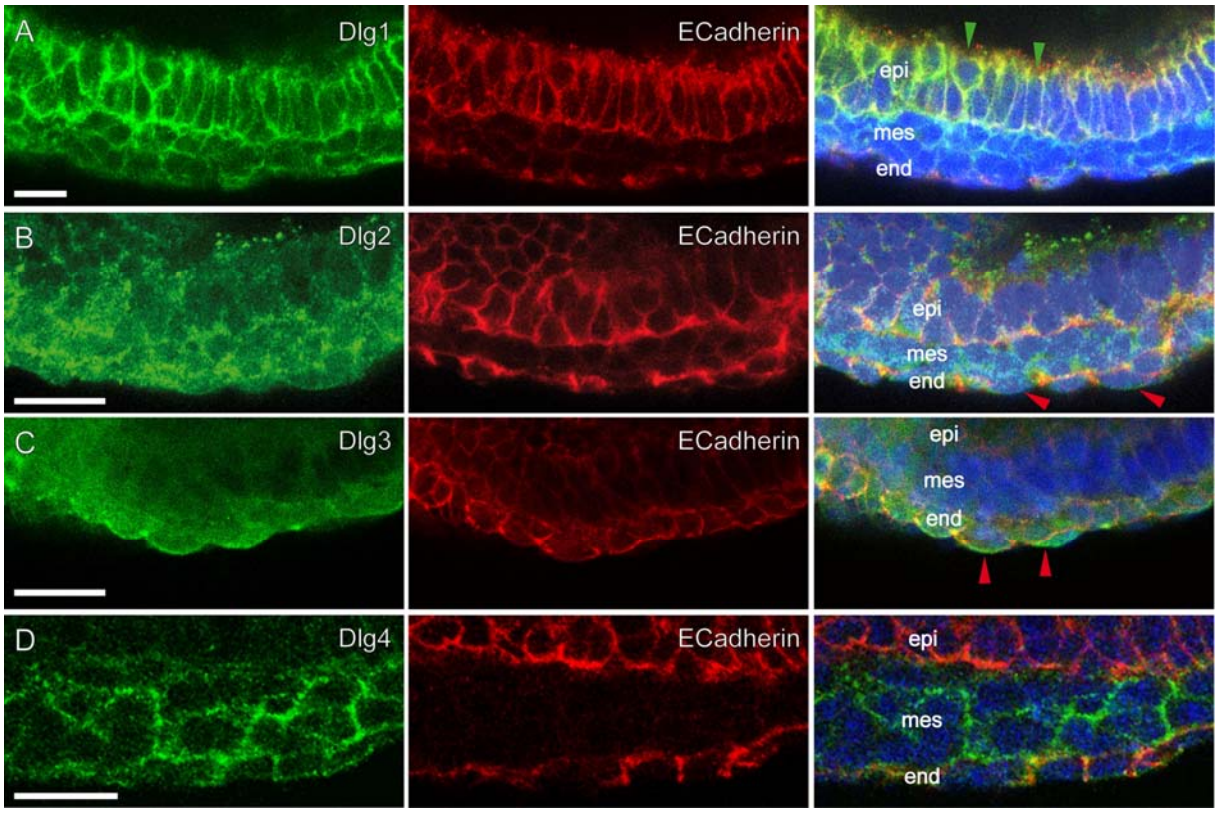

Figure S3. The mammalian Dlg1-4 present distinct cellular and subcellular localizations

(**A**-**D**) Whole mount colocalization studies of the Dlg proteins and the AJ marker E-cadherin in the different embryonic germ layers: epiblast (epi), mesoderm (mes) and endoderm (end) at E7.5. (**A**) Note the specific basolateral expression of Dlg1 in the epiblast and endoderm (marked by green arrowheads). (**B** and **C**) Dlg2 and 3 are found in the cytoplasm and the apical PM (red arrowheads). Scale bars = 20µm.

Figure S4, related to Figure 4

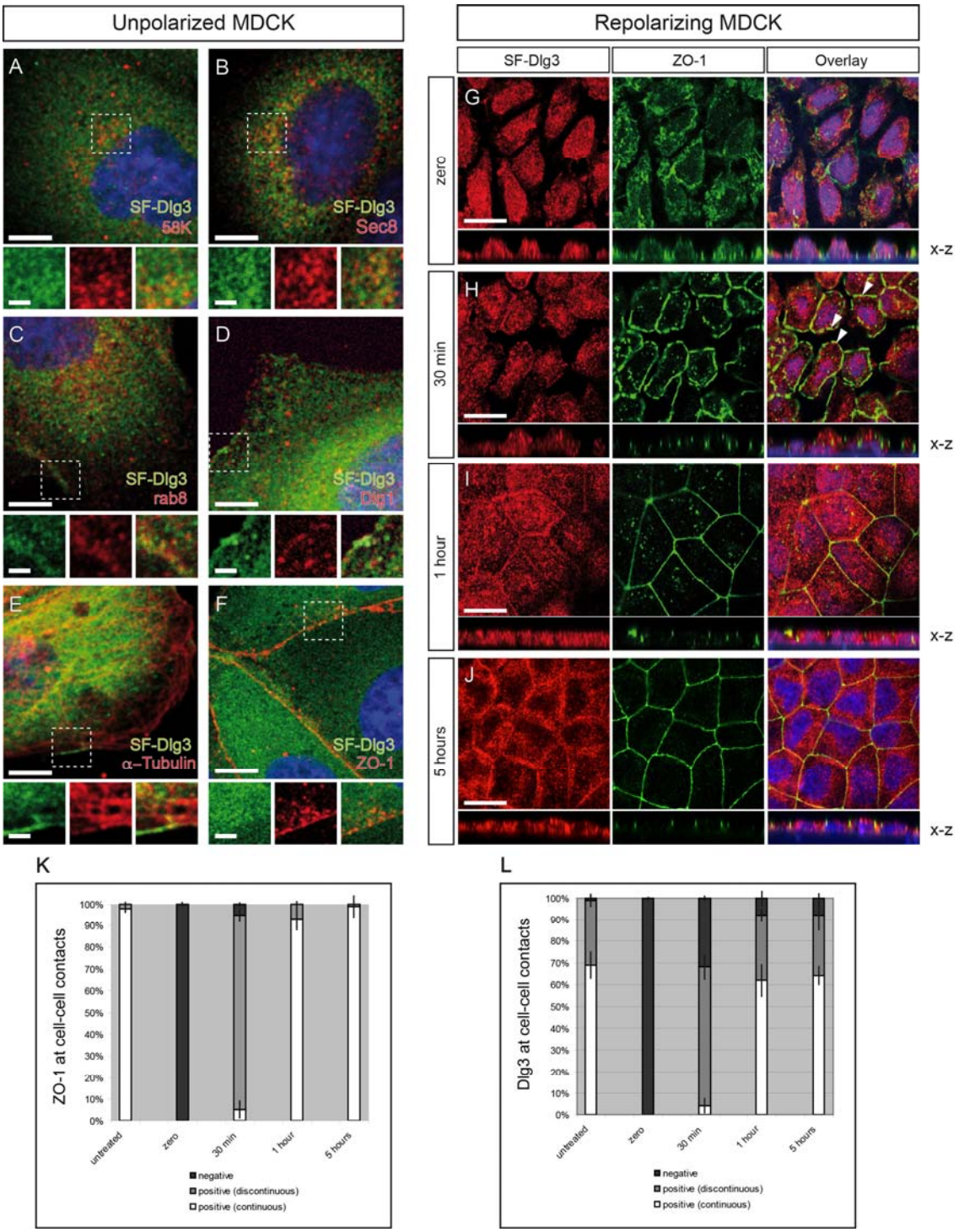

Figure S4. Dlg3 is recruited to the plasma membrane upon polarization

(**A-F**) Unpolarized stable SF-Dlg3 MDCK transfectants were stained with the specified antibodies and DAPI to mark the nuclei. (**A**) SF-Dlg3 colocalizes with the Golgi marker 58K, (**B**) with the exocyst component Sec8 and (**C**) the small GTPase Rab8. (**E**) SF-Dlg3 localizes

along microtubules, (**D**) to the cell membrane and (**F**) forming TJ. Scale bars = 50µm in (**A-F**) and 0.5µm in the higher magnification images.

(**G-J**) Repolarization/Ca^{2+}-switch assay. Polarized MDCK cells were incubated for 1 hour in medium deprived of Ca^{2+} and then incubated in a Ca^{2+}-containing medium for the indicated times. (**G**) Note that in the absence of Ca^{2+}, SF-Dlg3 localizes in the cytoplasm. (**H**) Already 30 min after addition of Ca^{2+}-containing medium, ZO-1 and SF-Dlg3 are recruited to the apical membrane and forming TJ (white arrowheads). (**I**) One and five (**J**) hours after Ca^{2+} addition, TJ are almost completely restored and SF-Dlg3 colocalizes with the TJ marker ZO-1. Scale bars = 10µm in (**G-J**).

(**K-L**) Quantification of ZO-1 (**K**) and Dlg3 (**L**) recruitment at cell-cell contacts in three independent repolarization/Ca^{2+}-switch assays. Cell-cell contacts were classified in three different categories based on ZO-1 and Dlg3 stainings: negative, discontinuous signal and continuous signal. 500 cell-cell contacts counted per experiment. Mean ± SD. Error bars indicate standard deviation.

Figure S5, related to Figure 5

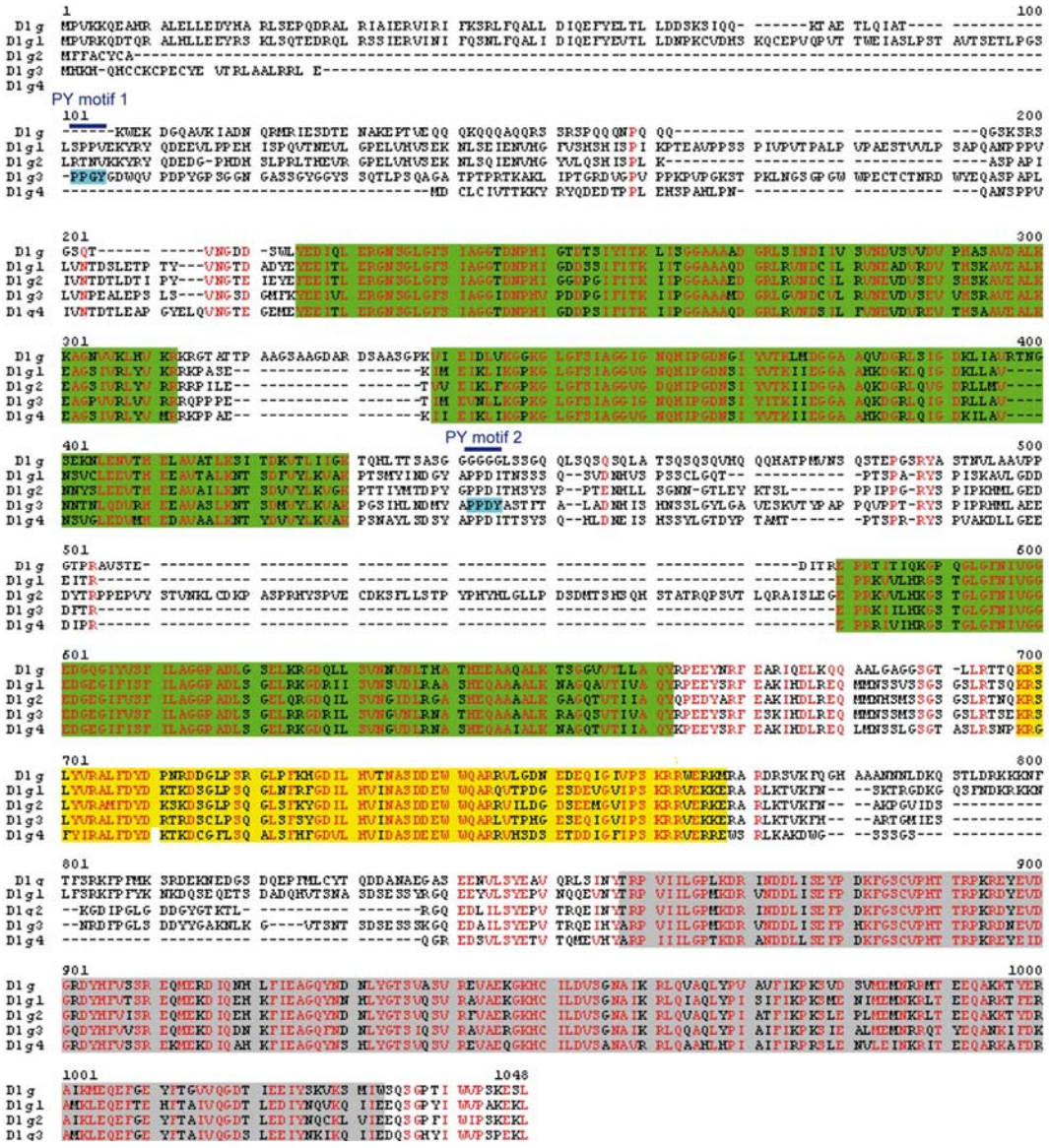

Figure S5. Dlg3, but not Dlg1, 2 and 4, contains PY motifs

Multiple species ClustalW alignment of the *Drosophila* Dlg and the mammalian Dlgs showing the presence of the PY motifs (blue) only in Dlg3. PDZ, SH3 and GUK domains are highlighted in green, yellow and grey respectively.

Figure S6, related to Figure 6

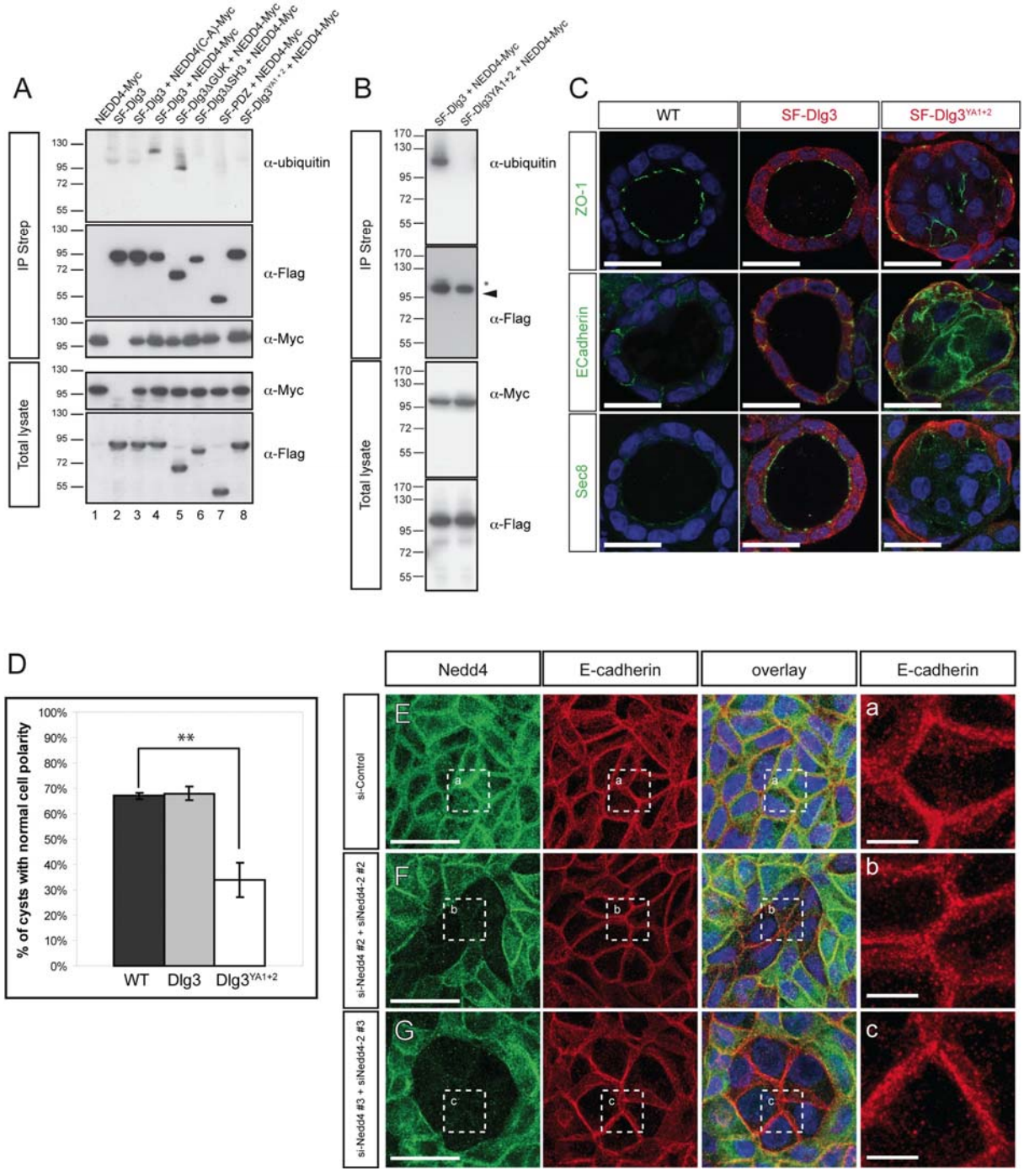

Figure S6. Nedd4 directly targets Dlg3 monoubiquitination and regulates its function

(**A**) *In vitro* monoubiquitination of Dlg3. HEK293T cells were transfected with the indicated constructs and immunoprecipitated with Strep affinity beads. Precipitates (IP Strep) were analyzed for ubiquitination by Western blotting. Expression of the different constructs (total lysate) was controlled by Western blotting. Note that in the presence of Nedd4-Myc (lane 4),

SF-Dlg3 in monoubiquitinated whereas the catalytically inactive Nedd4 (C-A)-Myc (lane 3) SF-Dlg3 is not modified. The monoubiquitinated subfraction can also be seen on the anti-Flag blot upon longer exposure (data not shown).

(**B**) *In vitro* monoubiquitination of Dlg3. HEK293T cells were transfected with the indicated constructs. Cells were lysed in 0.8% SDS containing buffer and boiled for 5 minutes. Samples were then diluted to 0.1% SDS prior to Strep IP. Precipitates (IP Strep) were analyzed for ubiquitination by Western blotting. Expression of the different constructs (total lysate) was controlled by Western blotting.

(C-D) Overexpression of SF-Dlg3^{YA1+2}, contrary to SF-Dlg3, impairs cell polarity and cell junction formation in MDCK cysts. Different MDCK cells lines of stable transfectants were used to derive six days old cysts and stained with cell junction markers. (**C**) Dlg3^{YA1+2} cysts showed altered morphology and mis-localized TJ (ZO-1, Sec8) and AJ (E-cadherin) markers. Scale bars= 25µm. (**D**) Compiled data from three independent experiments in which 400-500 cysts were counted. Mean ± SD; ** p <0.05. Error bars indicate standard deviation.

(**E-G**) Polarized MDCK cells were transiently transfected with a si-Control (**E**) or a combination of siRNAs targeting Nedd4 and Nedd4-2 (**F, G**). Cells were immunostained with anti-Nedd4 and anti-E-cadherin antibodies and analyzed by confocal microscopy. Boxed areas are shown in high resolution (**a-c**). (**F, G**) Note that the combined Nedd4 and Nedd4-2 knock down does not affect AJ formation. Scale bars= 25µm in (**E-G**) and 5µm in higher magnification images (**a-c**).

SUPPLEMENTAL EXPERERIMENTAL PROCEDURES

Tandem affinity purification and LC-MS/MS

SF-TAP tandem affinity purification and mass spectrometric identification have been performed as described previously (Gloeckner et al., 2007). Briefly, MDCK cell clones stably expressing SF-Dlg3 and control cells were lysed in TBS buffer (30 mM Tris-HCl pH 7.4, 150 mM NaCl) supplemented with 0.5% NP-40 (Roche), protease inhibitor cocktail (Roche) and phosphatase inhibitors (Cocktail I and II, Sigma) and the cell lysates were incubated with Strep-Tactin® Superflow® (IBA) for 1h. The affinity resin was washed three times with TBS buffer containing 0.1% NP-40 and eluted with desthiobiotin elution buffer (IBA) to obtain the first eluate. This eluate was then incubated with anti Flag M2 agarose (Sigma). After 3x washes of the affinity resin with TBS buffer containing 0.1% NP-40, the SF-Dlg3 was eluted by applying 200µl FLAG elution buffer containing 200 µg FLAG peptide (Sigma) dissolved in one ml TBS buffer. Prior to LC-MS/MS analysis, proteins were precipitated by Chloroform/Methanol precipitation and directly subjected to tryptic proteolysis overnight. When specified, only one purification step was applied via the STREP-tag. Mass spectrometric analysis of the samples was performed on an LTQ OrbitrapXL mass spectrometer (Thermo-Fisher) coupled to an Ultimate 3000 Nano-HPLC (Dionex). Database search was performed against the Uniref 100 database (date: 2008-06-19, 496237 entries) using the Mascot search engine (Matrix Science) with the following parameters: species restriction set to mammalian, trypsin as enzyme, 10 ppm as mass range for parent ions and 1 Da for fragment ions; carbamidomethyl as fixed modification and methionine oxidation and serine/threonine as well as tyrosine phosphorylation as variable modifications. Downstream analysis of the MS/MS-Data was performed using Scaffold (Proteome Software Inc.). For *in vitro* ubiquitination assay, Strep IP was performed as described earlier and Roti®-Load (Roth) was added to Strep-Tactin Superflow beads and boiled before western blot analysis.

Generation of expression vectors

All full length Dlgs were amplified by PCR and fragments were subcloned in the XhoI and NotI sites of the eukaryotic expression vector pCAGGS (Niwa et al., 1991) in frame with an N-term SF tag. Wild-type Nedd4-Myc and HECT mutant Nedd4 (C-A)-Myc were previously described (Scharschmidt et al., 2004). The different Dlg3 deletion mutants and point mutants were generated by PCR. The following primers were used:

Name	Sequence
Dlg1-FL-FWD	5´ TATGCCGGTCCGGAAGCAAGAT 3´
Dlg1-FL-REV	5´ TCATAGCTTTTCTTTCGCTGGG 3´
Dlg2-FL-FWD	5´ ATGTTCTTTGCATGTTATTGTGCAC 3´
Dlg2-FL-REV	5´ TTATAACTTCTCCTTTGAGGGAATCC 3´
Dlg3-FL-FWD	5´GGCAGTGCCATGCACAAGCACCAGCACTGCTGT 3´
Dlg3-FL-REV	5´ TCAGAGTTTTTCAGGGGATGGGAC 3´
Dlg4-FL-FWD	5´ ATGGACTGTCTCTGTATAGTGACAA 3´
Dlg4-FL-REV	5´ TCAGAGTCTCTCTCGGGCTG 3´
Dlg3-ΔPDZ-FWD	5´ CAGTATAGACCTGAAGAGTACA 3´
Dlg3-ΔPDZ-REV	5´ TCAGAGTTTTTCAGGGGATGG 3´
Dlg3-ΔSH3-FWD	5´ AAAAAGAGGGTGGAAAAGAAAGAGC 3´
Dlg3-ΔSH3-REV	5´ CAAGGACCTCTTCTCACTGGT 3´
Dlg3-ΔGUK-FWD	5´ ATGCACAAGCACCAGCACTGC 3´
Dlg3-ΔGUK-REV	5´ TTACCTGGCATAGTGAATTTCTTGT 3´
Dlg3-PDZ-FWD	5´ ATGCACAAGCACCAGCACTGCT 3´
Dlg3-PDZ-REV	5´CTGGGCCACAATGGTGACTGAC 3´
PY-motif 1-FWD	5´ CTTGAGCCTCCTGGCGCCGGGGACTGGCAG 3´
PY-motif 1-REV	5´ CTGCCAGTCCCCGGCGCCAGGAGGCTCAAG 3´
PY-motif 2-FWD	5´ ATGTATGCTCCCCCTGACGCTGCCAGCACTT 3´
PY-motif 2-REV	5´ AAGTGCTGGCAGCGTCAGGGGGAGCATACAT 3´

Whole mount *in situ* hybridization and RT-PCR

Whole mount *in situ* hybridization was performed as previously described (Lickert et al., 2001). The antisense RNA probes for the four *Dlgs* were transcribed from the 3´ UTR of sequence-verified cDNA clones and sense probes were used as the control. Fragments of 3´ UTR (500 bp to 1 kb long) were amplified by PCR and subcloned into pBluescriptKS-. Embryos were photographed using a Zeiss Stereo Lumar V12 microscope. For RT-PCR,

RNA was isolated from embryos using TRIzol® (Invitrogen) and dissolved in DEPC water. 2 µg of total RNA were used for reverse transcription which was performed with the SuperScript™ II Reverse Transcriptase kit (Invitrogen) and primed with random octamers.

The following primers were used:

Name	Sequence
Dlg1-3´UTR-FWD	5´ AGACGGATGTTGTTCTTTCTTTTTTC 3´
Dlg1-3´UTR-REV	5´ ATGAAATCATTACTTTAATAGCAG 3´,
Dlg2-3´UTR-FWD	5´ CAGTCACGACGTGTAAACGACGAGCA 3´
Dlg2-3´UTR-REV	5´ TTTCGATGGCAGCGGGCAGTGA 3´
Dlg3-3´UTR-FWD	5´ CCTACCCTGTACTGCGGCTT 3´
Dlg3-3´UTR-REV	5 ´ACAGCTCACCAGTAAGCGAG 3´
Dlg4-3´UTR-FWD	5´ AGAGACTCTGATTCCTGCCC 3´
Dlg4-3´UTR-REV	5´ ATACGCGCTTGGTCCCACCG 3´.
Dlg1-RT-FWD	5´TGTAGCAATCATGGCAGTGGGAAGG 3´
Dlg1-RT-REV	5´CACCGGACACTTGTCTTTTCAC 3´
Dlg2-RT-FWD	5´ GTGGTGAGGGACGCACTTTG 3´
Dlg2-RT-REV	5´ GCCTATGTGCTGGTTGACTGC 3´
Dlg3-RT-FWD	5´ GGCAGTCGTTCCTGTGCAGAAAAG 3´
Dlg3-RT-REV	5´GCCAGGCCTAAGTTACCGCTGTATC 3´
Dlg4-RT-FWD	5´ ACCCTAGCCTTTCTTCCCACCCTTC 3´,
Dlg4-RT-REV	5´GTCTTAAGGAGCAAGGGCTCGGAAC 3´
β-Actin-RT-FWD	5´ GACGAGGCCCAGAGCAAGAG 3´
β-Actin-RT-REV	5´ ATCTCCTTCTGCATCCTGTC 3´

Cell culture

HEK293(T) and MDCK cells were cultured using standard procedures. Stable transfection of MDCK cells was carried out using Transfectin™ (Biorad) and selection for Puromycin resistance (Puromycin 1 µg/ml). For cyst derivation, MDCK cysts were grown in Matrigel™ (BD; 2.10^6 cells/ml) for 5 days. Unpolarized and polarized MDCK cells were grown as previously described (Jaulin et al., 2007). For immunofluorescence, MDCK were seeded ($2,5.10^5$ cells/cm^2) on Transwell® filters (Corning) according to the manufacturer's instructions and cultured for 2 to 5 days. For repolarization/Ca^{2+} switch assays, MDCK cells were polarized on Transwells® filters for 2 days, washed several times in PBS, incubated for

one hour in low Ca^{2+} containing medium (S-MEM; Invitrogen) and then incubated with normal medium before fixation at different time points as indicated. Double-stranded siRNAs targeting dog *Nedd4* and *Nedd4-2* were purchased from Eurogentec.

The following sequences were used:

Name	Sequence
Nedd4 pair 1:	5´ GAUAAACUGCAGAUGGCAA 3´
Nedd4 pair 1:	5´ GGGAAGAGAGGCAGGAUAU 3´
Nedd4 pair 1:	5´ CAGAAAUAGUUGUCACCAA 3´
Nedd4-2 pair 2:	5´ CAGAAAUAAUGGUGACAAA 3´
Nedd4-2 pair 2:	5´ GGGAAGAGAAGGUGGACAA 3´
Nedd4-2 pair 2:	5´ AGAGAAAGGUCUUGACUAU 3´
Non targeting Control:	5´ CCAUCCUGAUGUCGCAAUA 3´

MDCK cells were transfected on Tranwells® filters with with siLentFect™ (Biorad) and 40 nM total siRNA oligos. Cells were fixed 72 hours after transfection.

Supplemental references

Jaulin, F., Xue, X., Rodriguez-Boulan, E., and Kreitzer, G. (2007). Polarization-dependent selective transport to the apical membrane by KIF5B in MDCK cells. Dev. Cell *13*, 511–522.

Lickert, H., Kispert, A., Kutsch, S., and Kemler, R. (2001). Expression patterns of Wnt genes in mouse gut development. Mech. Dev. *105*, 181–184.

Niwa, H., Yamamura, K., and Miyazaki, J. (1991). Efficient selection for high-expression transfectants with a novel eukaryotic vector. Gene *108*, 193–199.

Scharschmidt, E., Wegener, E., Heissmeyer, V., Rao, A., and Krappmann, D. (2004). Degradation of Bcl10 induced by T-cell activation negatively regulates NF-kappa B signaling. Mol. Cell. Biol. *24*, 3860–3873.